Green Touchable Nanorobotic Sensor Networks

Yifan Chen, *Senior Member, IEEE,* Tadashi Nakano, *Member, IEEE,* Panagiotis Kosmas, *Senior Member, IEEE,* Chau Yuen, *Senior Member, IEEE,* Athanasios V. Vasilakos, *Senior Member, IEEE,* and Muhamad Asvial, *Member, IEEE*

Abstract

Recent advancements in biological nanomachines have motivated the research on nanorobotic sensor networks (NSNs), where the nanorobots are *green* (i.e., biocompatible and biodegradable) and *touchable* (i.e., externally controllable and continuously trackable). In the former aspect, NSNs will dissolve in an aqueous environment after finishing designated tasks and are harmless to environment. In the latter aspect, NSNs employ cross-scale interfaces to interconnect the *in vivo* environment and its external environment. Specifically, the in-messaging and out-messaging interfaces for nanorobots to interact with a macro-unit are defined. The propagation and transient characteristics of nanorobots are described based upon the existing experimental results. Furthermore, planning of nanorobot paths is discussed by taking into account the effectiveness of region-of-interest detection and the period of surveillance. Finally, a case study on how NSNs may be applied to microwave breast cancer detection is presented.

This work was supported by the National Natural Science Foundation of China (61550110244), the Guangdong Natural Science Funds (S2013050014223, 2016A030313640), the Shenzhen Development and Reform Commission Funds ([2015]863, [2015]1939), and the Shenzhen Science, Technology and Innovation Commission Funds (KQCX2015033110182368).

Y. Chen is with the Department of Electrical and Electronic Engineering, Southern University of Science and Technology, Shenzhen, China (e-mail: chen.yf@sustc.edu.cn).

T. Nakano is with the Institute for Academic Initiatives, Osaka University, Osaka, Japan (e-mail: tadasi.nakano@fbs.osaka-u.ac.jp).

P. Kosmas is with the School of Natural and Mathematical Sciences, King's College London, London, United Kingdom (e-mail: panagiotis.kosmas@kcl.ac.uk).

C. Yuen is with Singapore University of Technology and Design, Singapore (e-mail: yuenchau@sutd.edu.sg).

A. V. Vasilakos is with the Department of Computer Science, Lulea University of Technology, Lulea, Sweden (e-mail: vasilako@ath.forthnet.gr).

M. Asvial is with the Department of Electronic Engineering, University of Indonesia, Depok, Indonesia (e-mail: asvial@ee.ui.ac.id).

I. Introduction

A. Background and Motivation

Recent progress in bio-nanomachines have motivated the research on bio-inspired, biocompatible, and biodegradable nanorobots such as flagellated magnetotactic bacteria (MTB) with nanometer-sized magnetosomes. These bacteria can be utilized as efficient carriers of nanoloads and thus can serve as diagnostic and therapeutic agents for tumor targeting applications [1], [2]. For example, the experiments in [2] demonstrated MTB targeted in the interstitial region of a tumor from the blood vessels. Moreover, it has been shown that MTB can be maneuvered by a magnetic field generated in custom-made MRI systems [1], [2]. Other examples of bio-nanorobots include motor proteins reconstructed for transportation of molecules, cells genetically modified for active moving, and so on [3].

These emerging technologies have motivated the design of nanorobotic sensor networks (NSNs) for detection and examination of regions-of-interest (ROIs) in an *in vivo* environment such as the internal space of the human body [4]. An NSN is comprised of a swarm of nanorobots, which are designed, engineered, and controlled to perform specific tasks such as adjusting the direction of movement based on an external propulsion-and-steering gradient, releasing signalling particles to form a concentration gradient, binding to particular cell receptors on the ROIs, and so on. The presence of ROIs is assumed to be a potential threat to the *in vivo* environment (e.g., tissue malignancies). The primary concern of NSNs is therefore to coordinate the movement of nanorobots and plan their paths, detect ROIs and identify their locations, and examine the properties (e.g., size and shape) of ROIs.

Information exchange between NSN and a macroscale monitoring device can be realized through cross-length-scale communication interfaces as to be presented in the current work. Furthermore, the degradability of nanorobots that contributes to “green” systems by allowing for benign integration into life will also be discussed.

B. Main Contributions

The main contributions of this work are as follows. First, due to size and power constraints, reliable direct communications between multiple nanorobots are difficult to achieve. Thus, one of the key strategies we propose here is to realize *touchable* NSNs by establishing interfaces to interconnect the small-scale aqueous environment and the large-scale non-aqueous environment. Such interfaces should allow an external macro-unit to control the timing of *in vivo* sensing processes taking place (i.e., start to release nanorobots) and the pathways of nanorobots, which expands the capability of NSNs. Subsequently, the

cross-scale in-messaging interface (IMI) and out-messaging interface (OMI) for nanorobots to interact with a macro-unit are presented, which facilitate the control, tracking, and sensing operations. The term "touchable" represents that the sensing process can be controlled and tracked. This is similar to controlling through simple or multi-touch gestures by touching the screen with a finger through a touchscreen, where the finger here refers to the external guiding field. The second important strategy we propose here is to realize *green* NSNs. This paradigm requires that each nanorobot dissolves into biofluids in the human body without creating harmful byproducts after carrying out the medical operations. Based on this strategy, empirical models of nanorobot bioresorbability based on experimental findings reported in [1], [2] are presented. Furthermore, planning of nanorobot paths is discussed by considering the effectiveness of ROI detection and the period of surveillance. The path optimization process contributes to green NSNs by reducing the time when nanorobots are present in the human body.

It is worth noting that the classical green networks are mostly focused on energy-relevant green issues. The current work, on the other hand, extends this conventional concept to include reduction of the use and generation of toxic substances. The green NSNs may also find important applications in environmental protection and monitoring, where system degradability allows for benign integration into environment.

The green touchable NSNs have potential to alleviate some of the limitations in the existing nanoscale communication paradigms [5], [6]. For example, nanosensors cannot store and process a large amount of data, change signalling particles at will, or control the particle release and reception processes accurately for the message encoding and decoding. Furthermore, there is a great deal of uncertainty during the propagation process caused by random Brownian motions, temperature variation, chemical reactions, molecule decomposition, and so on. The proposed system, on the other hand, only requires simple functionalities including sensing and manoeuvering at nanorobots, and moves most operations to a macro-unit. Moreover, remote controllability and trackability of nanorobots reduce propagation delay and eliminate environmental uncertainty.

The remainder of the paper is organized as follows. Section II gives an architecture of touchable NSNs. Section III describes the propagation and transient (i.e., "green") characteristics of nanorobots, while Section IV presents the path planning criteria. Section V illustrates the approach with an example of NSN for microwave breast cancer detection. Finally, some conclusions are drawn in Section VI.

II. System Architecture of Touchable NSNs

An architecture of touchable NSNs consists of remotely controllable and trackable nanorobots in an *in vivo* aqueous environment (e.g., blood vessels in the human body), and a macro-unit located in an

external environment (e.g., a hybrid operating room equipped with medical imaging devices). A macro-unit implements two types of interfaces: IMI and OMI (I/OMI), as shown in Fig. 1. It uses IMIs to transmit in-messages to nanorobots and OMIs to receive out-messages from nanorobots. Note that the communication interface for direct interaction between nanorobots is not implemented due to the limited size and computational power of nanoscale entities. The key components of touchable NSNs are described as follows.

A. Macro-unit and Nanorobot

A macro-unit is a large-scale device that relies on conventional means of controlling and imaging, which may be composed of materials incompatible with the *in vivo* environment and may be larger than nanorobots by orders of magnitude. A macro-unit can generate in-messages to and receive out-messages from nanorobots that reside in the *in vivo* environment. It consists of two main modules: the tracking module uses a medical imaging platform such as an optical microscope, a fluoroscopic system, an MRI machine, or a microwave imaging device [1], [2], [7] to monitor the movement and aggregation of nanorobots; the controlling module uses a traditional electronic, magnetic or optical system to release, propel or steer nanorobots.

A nanorobot is composed of biocompatible and biodegradable materials (e.g., MTB [1], [2]), and has a size ranging from the size of a macromolecule to that of a biological cell [3], [8]. A nanorobot implements the following basic functionalities [8]: *steering wheel* and *propeller* controlling respectively the swimming direction and speed of nanorobot, *fuel* unit harvesting energy from the surroundings to provide power to nanorobot, *sensor* unit acting as the interface between the aqueous medium and nanorobot, *nanoload* made of nanocomposites such as diagnostic agents and therapeutic drugs attached to nanorobot, and *navigator* tracking the movement of nanorobot. Examples of nanorobots include unicellular organisms, genetically modified cells, and biological cells [1]–[3], which are able to swim in the *in vivo* environment under the maneuver of an external field, carrying a cargo such as nanoparticles, acting as biosensors detecting specific molecules, and being integrated with cell-native components (e.g., magnetosomes in MTB) or coated with artificial materials (e.g., fluorescent molecules) for controlling and tracking purposes.

B. IMIs and OMIs

A macro-unit implements cross-scale IMIs and OMIs to interact with nanorobots as shown in Fig. 1. The IMIs must convert conventional electronic, magnetic, or optical signals used by the large-scale device into commands to which nanorobots respond by performing subsequent small-scale operations,

while the OMIs must convert motion signals generated by nanorobots (e.g., releasing, swimming, and targeting of nanorobots) to externally detectable and interpretable messages. Examples of IMIs and OMIs are as follows (see also Fig. 1).

The source IMI controls the release of nanorobots at a specified location and time from the nanorobot source [1]–[3], which initializes the sensing process. For example, a laser emits light at a specific frequency, which may cause caged compounds to release encapsulated molecules through bond breaking [3]. An MRI device generates a magnetic gradient, which may maneuver a swarm of MTB confined within an aggregation zone (AZ) towards a targeted destination by magnetotaxis [1], [2]. The source OMI tracks the release of nanorobots. For example, fluorophores such as derivatives of rhodmamine attached to nanorobots may emit light at a specific frequency in response to excitation from an external macro-unit and the macro-unit may detect emitted fluorescence [3]; an X-ray scanner may provide an angiogram showing the blood vessels for monitoring of catheter placements where a catheter is used to release nanorobots at a site near the target [1], [2].

The channel IMI controls the movement of nanorobots in the *in vivo* environment. First, an external macro-unit creates a propelling-and-steering field in the surveillance area as illustrated in Fig. 1. For example, in [1], [2], the patient was positioned inside the bore of an MRI system where MTB were released from the tip of a catheter. The maneuver of MTB required three-dimensional steering magnetic coils, which induced a torque on the chain of magnetosomes in MTB. In [1], [2], an agglomeration of MTB were controlled to move along predesigned microchannels mimicking the human microvasculature. The channel OMI tracks the path of nanorobots through various imaging modalities such as MRI (for MTB propagating in microvasculature) [1], [2] and fluorescence microscopy (for molecules propagating through gap junction channels) [3]. It is worth noting that propagating molecules themselves are not nanorobots. However, similar fluorescent technique can be applied to nanorobots for tracking purpose. In addition, differential microwave imaging can be employed for tracking of nanorobots, where the nanoload attached to nanorobots is a contrast agent such as carbon nanotubes [7], [9].

The ROI IMI controls the targeting, absorption, and dissolution of nanorobots at the ROI, while the ROI OMI tracks these processes occurring at the ROI, which also indicates the presence of ROI. Firstly, the nanorobots are not located until they reach an intermediate AZ. This is to avoid interference caused by electromagnetic fields generated during the propelling-and-steering phase and the tracking phase, as well as reduce the complexity of macro-unit. Furthermore, nanorobots in a swarm swim at different velocities during traveling to an AZ and as such they disperse, making the density too low for tracking (see e.g., [1], [2]). The distribution and number of AZs are dependent on the performance requirements of the

ROI sensing. Denser placement of AZs gives rise to more effective ROI detection and more accurate localization, at the cost of a longer surveillance period. Consequently, the measured nanorobot footprints corresponding to these AZs result in snapshots of the actual nanorobot paths. If a swarm of nanorobots fail to detect a ROI (i.e., the corresponding path does not cross the ROI), they will keep navigating until being maneuvered out of the surveillance area or dissolving in the medium. On the other hand, if these nanorobots reach a ROI, the nanoload will be removed and get assimilated into the ROI allowing the nanoload to carry out medical tasks. The attachment of the load to the ROI turns off the "navigator" module in the nanorobots. This may be realized by load discharging where the load itself also serves as the "navigator" (e.g., fluorescent molecules are only appended to the load). Consequently, the nanorobots will become invisible to the macro-unit. The final location of the nanoload will result in a "sink" on the preplanned nanorobot pathway as shown in Fig. 1.

Nanorobots can also be administered to target a detected and localized ROI from various directions through the ROI IMI [7]. In this case, the size and shape of the ROI can be estimated *via* registration of all the final nanorobot footprints as also shown in Fig. 1. This additional information will help reduce false alarms for ROI inspection. The information about the properties of a ROI is thus achieved by requiring the macro-unit to observe the footprints of nanorobots. This *seeing-is-sensing* strategy forms the ROI OMI of the touchable NSN. It is worth noting that the sensing operation can be combined with targeted transportation of nanocomposites to the ROI, while preventing them from affecting other sites within the surveillance area. An important application is targeted drug delivery, which enhances locoregional therapies for cancer treatment without causing toxic effects to non-targeted sites in the human body.

III. Propagation Characteristics and Transient Kinetics of Nanorobots for Green NSNs

A. Propagation Models of Nanorobots

1) Velocity-Jump Random Walk Model: Nanorobots under the guidance of externally exerted magnetic fields resulted in trajectories similar to random walks as demonstrated in [10]. Various random walk models for different molecular propagation scenarios have been discussed in [11]. In [12], a velocity-jump random walk process was employed for simulating the nanorobot movement in a liquid along the propelling field lines. According to this model, nanorobots move forward with a time-varying velocity for a random step, which follows a Poisson process of turning frequency λ. To model changes in direction, a von Mises distribution of mean θ and concentration κ is employed. The mean of this distribution depends on the propelling field at the present location and thus introduces a directional bias. The width

of the angular spread increases as κ reduces. The two parameters λ and κ characterize the effects of microenvironmental mechanisms (e.g., chemotaxis and aerotaxis) and the propagation environment. A large λ indicates a small mean run length time, which is applicable to a homogeneous fluid medium that lacks a flux structure imposing constraints on the feasible nanorobot paths. In this case, $1/\lambda$ is mainly controlled by the curvature of the external field line. On the other hand, a small λ corresponds to a structured fluid network, in which nanorobots will travel through the fluid vessels and will not change their direction frequently. In this scenario, $1/\lambda$ is related to the average length of each straight section of the flow network, such as a branch in the vascular tree. Furthermore, a large κ indicates that the propelling force predominates over other microenvironmental gradients. In general, a flux structure also leads to a small κ.

2) Fractal-Based Statistical Model: The pathway of nanorobots may also be described using the fractal-based statistical model [8], which characterizes the movement of nanorobots in a vascular tree when the capillaries can be imaged. Firstly, the vascular network distributes the blood stream through the human body by successive bifurcations, which can be described by a fractal model due to the self-similar character of a bifurcating tree. Secondly, the hemodynamic response leads to increased cross-sectional areas of blood flow, which results in blood velocity low enough for the exchange of metabolic substances across the capillary wall. The hemodynamics explains the empirical Murray's laws that characterize the connection between the diameter of the parent segment and the diameters of two daughter branches at each bifurcating node [8]. The angle between two daughter vessels after division and the lengths of the vessels are also determined by the Murray's formula. Finally, when the microvasculature becomes angiographically unresolvable, it may be simplified as a structureless fluid medium and the velocity-jump random walk mentioned above may be used to describe the pathway of nanorobots as suggested in [8].

3) Deterministic Model: The pathway of nanorobots may also be described using the deterministic topology of large arteries collected from anatomical data [13]. The model in [13] was divided into two parts: the cardiovascular network model and the drug propagation network model. The former was obtained by solving the Navier-Stokes equation, which computed the blood velocity at an arbitrary location through the cardiovascular network given the blood pressure. In this case, the transmission line analysis was applied to characterize the arterial interconnection. The latter was obtained by solving the advection-diffusion equation, which computed the concentration of drug particles at an arbitrary location through the cardiovascular network given the blood velocity. In this case, the harmonic transfer matrix analysis was applied to characterize the transfer function of each blood vessel and dichotomous division.

B. Transient Kinetics of Nanorobots for Green NSNs

The degeneration of bacterial nanorobots (e.g., MTB) results in decrease in their terminal velocity. In [1], [2], Martel *et al.* measured the velocity of a large agglomeration of MTB by using a video camera mounted on an optical microscope. The velocity exhibited two-stage kinetics with respect to the immersion time for 37° blood temperature. If the threshold speed below which a bacterium is considered degenerating is $100\ \mu\mathrm{m/s}$, MTB would function stably for a duration of $15\ \mathrm{min}$. Over the following $25\ \mathrm{min}$, MTB started to deteriorate with gradual reduction in their speed. Overall, MTB remained active for $40\ \mathrm{min}$ and then slowed down due to high blood temperature. Moreover, it has been demonstrated that a swarm of MTB could be controlled like a single organism to swim along a predetermined path by an external computer [1], [2]. The amount of MTB in each swarm is usually large and therefore, it is useful to look into their concentration at various locations of blood vessels. As such, the transient behavior of MTB is also related to diffusion of bacteria in the medium. The diffusion effect has been commonly modeled by using the Fick's laws for space of various dimensions [8], [11]. Then, the overall transient characteristic of MTB (ranging between 0 and 1 for no resorption and complete resorption, respectively) is given by the percentage of diffused MTB on arrival at the ROI, if the total immersion time is less than the lifespan of MTB. Otherwise, the MTB are fully degenerated.

IV. Nanorobot Path Planning Criteria

Two criteria for nanorobot path planning are considered in this section, which are based on the effectiveness of ROI detection and the period of surveillance.

Consider a number of *sequential* and *directional* nanorobot routes in the *in vivo* environment to cover the entire surveillance area. Each route utilizes one set of nanorobots to cut through the surveillance area. If a ROI is identified and assuming that its spatial distribution is known *a priori* (e.g., *via* a lower-resolution tomographic image), the probability of the ROI being present within the area traveled by nanorobots between any two adjacent AZs, A_1 and A_2, can be estimated. The ROI detection between these two AZs aims to distinguish between the null hypothesis $\mathcal{H}_0$ ("ROI is absent") and the alternative hypothesis $\mathcal{H}_1$ ("ROI is present"). If $\mathcal{H}_1$ is true, a portion of the fluorescent nanoload will be successfully discharged, and the rest will be transported to A_2. Subsequently, the indicator quantity signifying presence or absence of nanoload at A_2 is the sum of the transient characteristic at A_2 without encountering any ROI, and the increase in transient characteristic due to nanoload unloading at the ROI between A_1 and A_2. Then, the probability of ROI detection is given by the probability that the indicator is no less than a pre-specified threshold beyond which nanorobot tracking would fail. If there is no ROI between A_1

and A_2, the indicating metric is given by the transient characteristic at A_2 without encountering any ROI. The probability of false alarm is obtained as the probability that the indicator is no less than the same threshold. Subsequently, the overall probabilities of detection and false alarm can be obtained. The Youden's index, which is the difference between the probabilities of detection and false alarm, can thus be calculated and the corresponding path planning criterion is to identify the optimal route such that the Youden's index is maximized. In general, optimal path planning rules should ensure that AZs where the ROI detection performance is poorer (i.e., smaller Youden's indices) should also correspond to areas with lower probabilities of ROI presence. Furthermore, to achieve more effective ROI detection, the direction of nanorobot movement for each path should be designed such that the location-variant nanorobot transient characteristics "match" the spatial distribution of ROI in the surveillance area (i.e., the denser the distribution of the ROI, the smaller the transient characteristic of nanorobots). In other words, the "higher-risk" areas should be surveyed when the nanorobots deployed are under more reliable operating conditions.

The second criterion for optimization of nanorobot paths is based on the time to ROI detection. Our goal is to identify the desirable set of paths resulting in cumulative distribution function of time-to-detection the maximum across all times. There are two general strategies to obtain the solution. First, if the spatial distribution of the ROI in the interior of the surveillance area is available, the preplanned nanorobot routes should "match" the probability map, such that the AZ begins with the location of the highest probability of ROI detection and shifts successively to locations having descending detection probabilities. This protocol is consistent with the strategy suggested previously because the transient characteristic is a non-decreasing function with the operation time. Second, the velocity should also "match" the probability map, where the nanorobots navigate across the areas having higher probabilities of ROI presence with higher speeds. Similarly, this condition agrees with the other strategies mentioned above because the velocity is a non-increasing function with the operation time [1], [2].

It is worth emphasizing that the path planning strategies also contribute to green NSNs by reducing the duration of the nanorobots' presence in the *in vivo* environment.

V. Case Study: NSN for Microwave Breast Cancer Detection

Microwave medical imaging for early-stage breast cancer diagnosis attempts to discriminate breast tissues based on their dielectric properties [7], [9]. However, its effectiveness is compromised by clutter interference due to healthy tissue inhomogeneities. This problem can be solved by using a contrast agent to change the tumor tissue dielectric values. The agent is transported selectively to cancer cells *via* systemic

administration for specific and non-invasive diagnosis of tissue malignancies. However, the existing targeting techniques have limited efficacy as a result of intratumoral penetration limit. Consequently, only a small amount of contrast agent is able to enter cancer cells.

NSN can provide a potential remedy for the aforementioned problem. For example, suppose that MTB are used to deliver effectively a contrast agent (i.e., nanoload) to a tumoral region (i.e., ROI) in the human breast. Each time an agglomeration of MTB loaded with a contrast agent are injected into the breast (i.e., surveillance area) from a predefined injection site. The MTB will navigate towards the direction of an externally exerted magnetic field and their movement can be tracked by using a differential microwave imaging system (i.e., macro-unit) [7], [9]. When a particular swarm trajectory meets a tumor, the contrast agent will be discharged from the nanorobots and attached to cancer cell receptors (i.e., nanoload discharging). Subsequently, the unloaded nanorobots may no longer be trackable by the differential imaging system, which only detects difference in the tissue dielectric properties caused by the agent. Therefore, a nanorobot footprint "sink" inside the breast would emerge at the tumor location where the contrast agent accumulates eventually (i.e., seeing-is-sensing).

To elaborate on the approach, consider a "heterogeneously dense" numerical phantom in the breast model repository in [14], which also includes a tumor having the dielectric values of cancerous breast tissue. Similar to [7], [9], an antenna array consisting of 40 dipole elements arranged over 5 circular rings is employed as the macro-unit. Two-dimensional tumor sensing along the cross-sectional planes of the rings is implemented using the differential microwave imaging data. For illustrative purpose, consider the cross-sectional plane slicing through the tumor. The corresponding dielectric profile is shown in Fig. 2(a). It is supposed that the presence of a contrast agent in a tissue region will substantially change its dielectric values [9]. Simulation studies on the movement, tracking, and location estimation of MTB have been presented in [7].

Assuming that the distribution of a cancer is given by the profile indicated in Fig. 2(a) (i.e., uniformly distributed within the high-dielectric-property areas encircled by the 3 dotted ellipses), the optimal MTB routes following the principles stated in Section IV are depicted in Fig. 2(a), and explained in the figure caption. Note that the sequence and direction of the MTB paths are determined by the criteria based on the detection effectiveness and surveillance period. More specifically, *the higher the distribution of ROI, the larger the Youden's index, the smaller the MTB transient characteristic, and the higher the MTB speed.* Fig. 2(b) shows a typical trajectory following the optimized survey route in Fig. 2(a). The velocity-jump random walk model is considered. An MTB footprint sink indicating the tumor location is registered. Fig. 3 shows the probability distributions of the tumor sensing time for both the optimized

and non-optimized scenarios when the number of simulation runs is 1000. In the latter case, the same survey paths are used but with a non-selective sequence and direction of traveling (i.e., left-to-right, up-to-down). As can be seen from the figure, in general the probability distribution when the MTB path is optimized decreases with the sensing time, whereas the distribution for the non-optimized situation is more uniformly distributed over the entire range of surveillance period. With path optimization, the mean and median values have been reduced from 27 min to 24 min, and from 23 min to 20 min, respectively.

VI. Conclusions

A novel system of green touchable NSNs has been introduced in this article. The system makes use of cross-scale IMIs and OMIs to facilitate the control, sensing, and transportation operations at the bottom. Nanorobots would disappear in the fluid medium after completing designated tasks, which eliminates the costs and environmental/health risks incurred by the retrieval of waste materials. The fundamental principles, propagation and degradation models, and design case study of the proposed system have been presented. Both environmental friendliness and path planning strategies help to realize green NSNs. The analytical framework presented here would pave the way for system-level implementations and experimental studies of NSNs in future.

References

[1] S. Martel, M. Mohammadi, O. Felfoul, Z. Lu, and P. Pouponneau, "Flagellated magnetotactic bacteria as contralled MRI-trackable propulsion and steering systems for medical nanorobots operating in the human microvasculature," *Int. J. Rob. Res.*, vol. 28, pp. 571–582, Apr. 2009.

[2] S. Martel, O. Felfoul, J.-B. Mathieu, A. Chanu, S. Tamaz, M. Mohammadi, M. Mankewich, and N. Tabatabaei, "MRI-based medical nanorobotic platform for the control of magnetic nanoparticles and flagellated bacteria for target interventions in human capillaries," *Int. J. Rob. Res.*, vol. 28, pp. 1169–1182, Sep. 2009.

[3] T. Nakano, S. Kobayashi, T. Suda, Y. Okaie, Y. Hiraoka, and T. Haraguchi, "Externally controllable molecular communication," *IEEE J. Sel. Areas Commun.*, vol. 32, no. 12, pp. 2417–2431, Dec. 2014.

[4] Y. Okaie, T. Nakano, T. Hara, and S. Nishio, "Autonomous mobile bionanosensor networks for target tracking: A two-dimensional model," *Nano Commun. Netw.*, vol. 5, pp. 63–71, 2014.

[5] S. F. Bush, *Nanoscale Communication Networks*, Artech House, 2010.

[6] I. F. Akyildiz, J. M. Jornet, and M. Pierobon, "Nanonetworks: A new frontier in communications," *Commun. ACMs*, vol. 54, pp. 84–89, Nov. 2011.

[7] Y. Chen, P. Kosmas, and S. Martel, "A feasibility study for microwave breast cancer detection using contrast-agent-loaded bacterial microbots," *Int. J. Antennas Propag.*, vol. 2013, Article ID 309703, 11 pages.

[8] Y. Chen, P. Kosmas, P. S. Anwar, and L. Huang, "A touch-communication framework for drug delivery based on a transient microbot system," *IEEE Trans. Nanobiosci.*, vol. 14, no. 4, pp. 397–408, June 2015.

[9] Y. Chen and P. Kosmas, "Detection and localization of tissue malignancy using contrast-enhanced microwave imaging: Exploring information theoretic criteria," *IEEE Trans. Biomed. Eng.*, vol. 59, no. 3, pp. 766–776, Mar. 2012.

[10] I. S. M. Khalil, M. P. Pichel, L. Abelmann, and S. Misra, "Closed-loop control of magnetotactic bacteria," *Int. J. Rob. Res.*, vol. 32, pp. 636–648, 2013.

[11] T. Nakano, M. J. Moore, F. Wei, A. V. Vasilakos, and J. Shuai, "Molecular communication and networking: Opportunities and challenges," *IEEE Trans. Nanobiosci.*, vol. 11, no. 2, pp. 135–148, June 2012.

[12] Y. Chen, P. Kosmas, and R. Wang, "Conceptual design and simulations of a nano-communication model for drug delivery based on a transient microbot system," in *Proc. 2014 8th European Conference on Antennas and Propagation (EuCAP)*, The Hague, The Netherlands, Apr. 2014, pp. 63–67.

[13] Y. Chahibi, M. Pierobon, S. O. Song, and I. F. Akyildiz, "A molecular communication system model for particulate drug delivery systems," *IEEE Trans. Nanobiosci.*, vol. 60, no. 12, pp. 3468–3483, Dec. 2013.

[14] E. Zastrow, S. K. Davis, M. Lazebnik, F. Kelcz, B. D. Van Veen, and S. C. Hagness, "Development of anatomically realistic numerical breast phantoms with accurate dielectric properties for modeling microwave interactions with the human breast," *IEEE Trans. Biomed. Eng.*, vol. 55, no. 12, pp. 2792–2800, Dec. 2008.

PLACE PHOTO HERE

Yifan Chen is presently a Professor and Head of Department of Electrical and Electronic Engineering with Southern University of Science and Technology, Shenzhen. His current research interests include transient communications, small-scale and cross-scale communications and sensing, microwave medical imaging and diagnosis, and propagation channel modelling. He is a key contributor to IEEE Std 1906.1 on Nanoscale and Molecular Communication Framework, and an Editor for IEEE ComSoc Best Readings in Nanoscale Communication Networks.

PLACE PHOTO HERE

Tadashi Nakano is an Associate Adjunct Professor of the Institute of Academic Initiatives, Osaka University, and a Guest Associate Professor of the Graduate School of Biological Sciences, Osaka University. His research interests are in the areas of network applications and distributed computing systems with strong emphasis on interdisciplinary approaches. His current research is focused on the Biological ICT including design, implementation, and evaluation of biologically inspired systems and synthetic biological systems.

PLACE PHOTO HERE

Panagiotis Kosmas is currently a Senior Lecturer at King's College London, Department of Informatics. He is also a co-founder of Mediwise Ltd, an award-winning UK-based SME focusing on the use of electromagnetic waves for medical applications. His research interests include bio-electromagnetics with application to wave propagation, sensing and imaging, antenna design, physics-based detection methods, and inverse problems theory and techniques.

PLACE PHOTO HERE

Chau Yuen was a postdoc fellow in Lucent Technologies Bell Labs during 2005. During the period of 2006-2010, he was at the Institute for Infocomm Research as a senior research engineer. He joined Singapore University of Technology and Design as an assistant professor from June 2010. He also serves as an associate editor for IEEE Transactions on Vehicular Technology. In 2012, he received the IEEE Asia-Pacific Outstanding Young Researcher Award.

PLACE PHOTO HERE

Athanasios V. Vasilakos is recently Professor with the Lulea University of Technology, Sweden. He served or is serving as an Editor for many technical journals, such as the IEEE Transactions on Network and Service Management; IEEE Transactions on Cloud Computing, IEEE Transactions on Information Forensics and Security, IEEE Transactions on Cybernetics; IEEE Transactions on NanoBioscience, IEEE Journal on Selected Areas in Communications. He is also General Chair of the European Alliances for Innovation.

PLACE PHOTO HERE

Muhamad Asvial is currently a researcher and lecturer at Electrical Engineering Department Universitas Indonesia. His research interests include mobile communication (terrestrial and satellite communication), HAPs Network, Genetic Algorithm Applications, Broadband and Ultra Wide Band Communication System. He published over 90 papers in several international journals and conferences. He is a member of the IEEE, the IET and the AIAA.

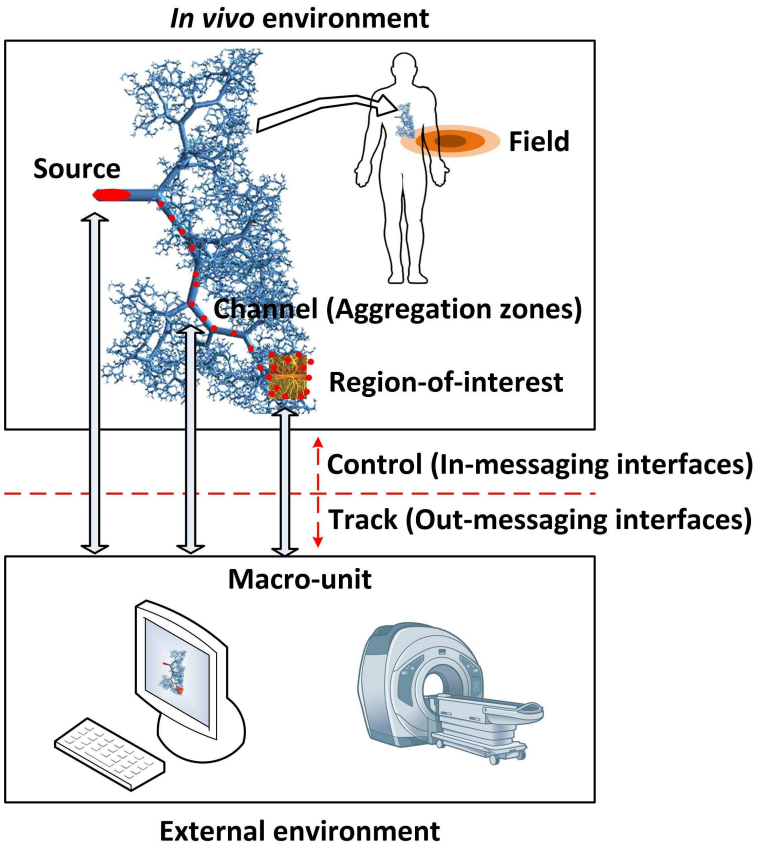

Fig. 1. An architecture of touchable nanorobotic sensor networks with in-messaging interfaces and out-messaging interfaces.

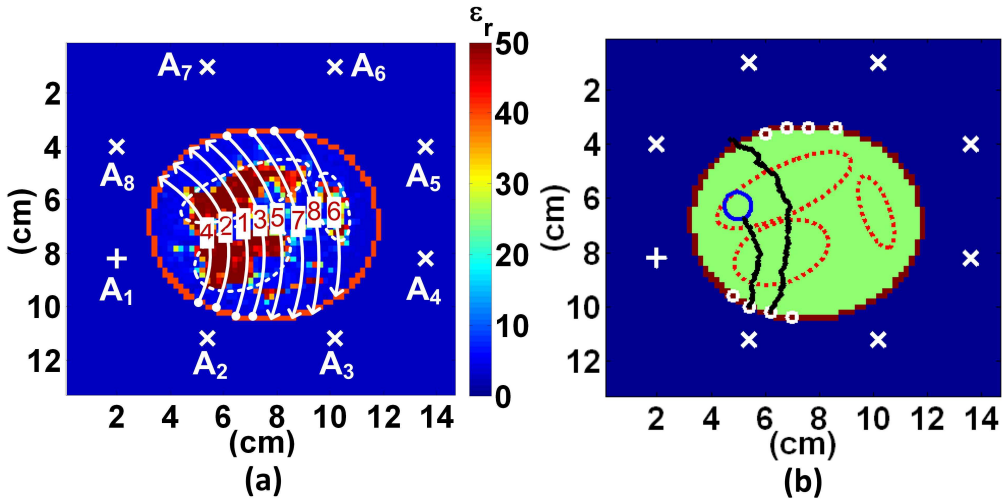

Fig. 2. (a) Dielectric profile of the breast cross-section at 1 GHz. A cancer is assumed to be uniformly distributed within the regions encircled by the 3 dotted ellipses. A dc source (marked with "+") generates concentric magnetic fields. The nanorobot survey routes (marked with white curved arrows) cover the surveillance area, which are designed by applying the path planning principles stated in Section IV. The arrow and number indicate the direction and sequence of the routes, respectively. (b) Simulated tumor location (marked with blue circle) and nanorobot trajectories (marked with thick black curves) following the optimized survey plan in (a).

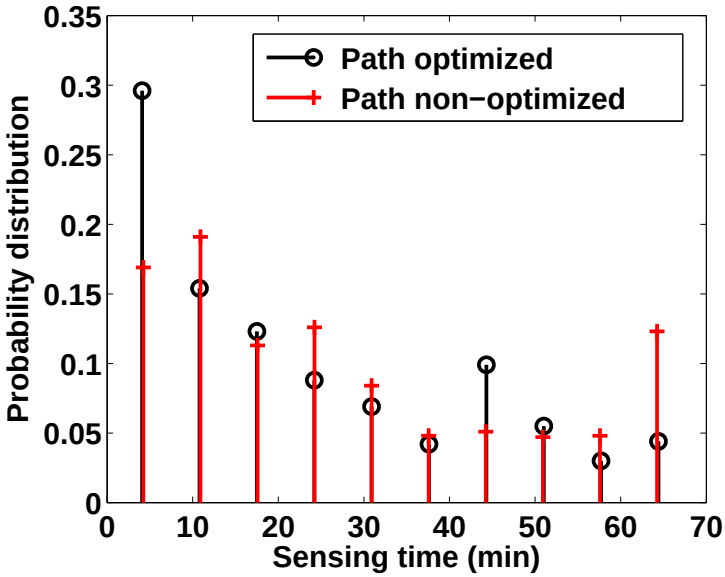

Fig. 3. The probability distributions of the sensing periods for the optimized and non-optimized nanorobot routes.